Am J Cancer Res 2022;12(8):3932-3946
www.ajcr.us /ISSN:2156-6976/ajcr0144792

Original Article

Snail induces dormancy in disseminated luminal type A breast cancer through Src inhibition

Chun-Te Ho[2*], Shih-Pei Lin[1*], Ling-Ming Tseng[3,4*], Mien-Chie Hung[5], Shih-Chieh Hung[1,2]

[1]Drug Development Center, Institute of New Drug Development, China Medical University, Taichung 404, Taiwan; [2]Integrative Stem Cell Center, Department of Orthopaedics, China Medical University Hospital, Taichung 404, Taiwan; [3]Department of Surgery, Taipei Veterans General Hospital, Taipei 112, Taiwan; [4]School of Medicine, College of Medicine, National Yang-Ming Chiao Tung University, Taipei 112, Taiwan; [5]Graduate Institute of Biomedical Sciences, Research Center for Cancer Biology and Center for Molecular Medicine, China Medical University, Taichung 404, Taiwan. [*]Equal contributors.

Received June 16, 2022, Accepted July 28, 2022; Epub August 15, 2022; Published August 30, 2022

Abstract: Breast cancer includes biologically distinct subtypes, and the time between rise in distant metastases and overall survival for the subtypes are different. The mechanisms involved in these differences in tumor metastasis remain to be elucidated. Here, we demonstrated that, luminal type A breast cancer cells, such as MCF7 and T47D, when overexpressed with active mutant form of Snail (6SA-Snail) increased in the expression of EMT markers such as Vimentin, N-cadherin and Fibronectin but decreased in the expression of E-cadherin, compared to control vectors or wild type Snail. Moreover, this mutant increased in migration and invasion ability, while decreased in the capacity to survive and form spheres in tumor spheroid medium. Luciferase reporter assay and chromatin immunoprecipitation followed by quantitative PCR (ChIP-qPCR) analysis revealed that Snail downregulated Src by binding to the E-box of Src promoter. Human luminal type A breast cancer specimens showed an inverse correlation between Vimentin and Src expression. Most importantly, downregulation of Src by Snail was not found in breast cancer cell types other than luminal type A. Therefore, elucidation of the differences in signaling pathways involved in controlling migration, invasion and colonization may have a therapeutically beneficial effect on breast cancer treatment.

Keywords: Breast cancer, luminal type A, colonization, suspension survival, Src, Snail

Introduction

Breast cancer, ranking the most common malignant disease in Western women, is classified into five biologically distinct subgroups including Luminal A (ER^+ ck8h/ck18h), Luminal B (ER^+ $ck8^l/ck18^l$), Basal (ER^- $ck5^+/ck17^+$) and $ERBB2^+$ (ER^- $ERBB2^+$ $GFRBP7^+$) and normal breast-like types. Luminal type has the best prognosis, while basal type or $ERBB2^+$ has the worst prognosis. Interestingly, basal type or $ERBB2^+$ breast cancers relapse and develop metastasis early (less than 5 years from surgery), while ER^+ cancers have a relative constant rate of relapse and metastasis over several years to decades, showing latency in cancer progression [1]. Although targeting ER signaling to modulate the DNA repair activities of BRCA1 [2] or inhibiting microtubules with 5-arylalkynyl-2-benzoyl thiophene [3], may induce cancer cell toxicity, these strategies may not prevent latent metastasis.

In breast cancer, metastasis rather than the primary tumor is the leading cause of death. According to the widely held model of metastasis, rare subpopulations of cells within the primary tumor acquire advantageous genetic alterations over time, which enable these cells to metastasize and form new solid tumors at distant sites [4]. Recently, metastasis is demonstratedasastep-wiseprocess,cooperatedbyepithelial-to-mesenchymal transition (EMT) wherein epithelial cells depolarize and gain the capacity for invasion, intravasation, survival in circulation and extravasation [5], whereas mesenchymal to epithelial transition (MET) manages disseminated cancer cells outgrowth for colonization [6].

Cancer dormancy, known as the latency period for cancer progression, in which residual disease is present but remains asymptomatic, may precede the development of recurrent metastatic disease for years or even decades [7]. There are various mechanisms of cancer dormancy including cellular dormancy (G0-G1 arrest) with reduced mitogenic or PI3K-AKT signaling, angiogenic dormancy, activation of stress signaling, microenvironmental regulation via secreted BMP4 or BMP7, and immunosurveillance [8-11]. However, these mechanisms fail to explain the differences in latency between different subtypes of mammary cancer. It is necessary to provide a new picture of how cancer dormancy occurs and how it could be a therapeutic target.

Pancreatic cancer cells that have undergone EMT and acquired stem cell properties can disseminate from primary neoplastic lesions [12]. Moreover, expression of EMT inducer, Snail or Twist [13, 14], induction of EMT by TGF-β [15], or the expression of jumping translocation breakpoint (JTB) gene [16] promotes dissemination and metastasis of mammary neoplasia. These data suggest that EMT may be responsible for dissemination. However, disseminated cancer cells (DCCs) still go through a latency period in which they acquire additional genetic or epigenetic changes to adapt and colonize. The metastatic microenvironments, in which metastatic lesions almost invariably display epithelial features, suggests that DCCs should undergo MET to adopt epithelial phenotypes before colonization [17].

Here, we hypothesized that cancer dormancy in different subtypes of mammary tumors may occur during EMT development. We first showed that prolonged latency in luminal A breast cancer was associated with loss of epithelial markers following EMT induction, which was not observed in other breast cancer subtypes. In luminal type A breast cancer, Snail$^+$ cells underwent EMT but lost the ability to colonize, which was attributed to Snail-induced Src downregulation. Only when the active form of Src was overexpressed, Snail$^+$ DCCs started to survive in suspension culture and form spheroids. Collectively, these data demonstrate that targeting the mechanisms of metastatic dormancy in breast cancer may lead to the development of new strategies for the treatment of this disease.

Materials and methods

Cell lines and reagents

MCF7, T47D and MDA-MB-231 cell lines were obtained from ATCC and grown in DMEM/F12 (Gibco, Grand Island, NY) containing 10% FBS. Other breast cancer cell lines AU-565 and BT-474 were obtained from ATCC and cultured in RPMI-1640 (Gibco) containing 10% FBS. All cells were cultured at 37°C in a humidified incubator containing 5% CO_2. Cell lines used in the study were confirmed to be mycoplasma-negative before experiments. The following reagents were purchased from commercial companies: PP2 (10 μM, Sigma-Aldrich, Saint Louis, MO), U0126 (20 μM, Sigma-Aldrich) and S3I-201 (100 μM, Merk, Schwalbach, Germany).

Western blotting assay

Cells (8×10^5) were rinsed with PBS and lysed by M-PER Mammalian Protein Extraction Reagent (Pierce, IL) with Halt™ Protease Inhibitor Cocktail Kit (Pierce, IL). Protein levels were determined using the BCA assay (Pierce, IL). After being heated for 5 min at 95°C in Laemmli Sample Buffer (Bio-rad, Richmond, CA), equal aliquots of the cell lysates were run on a 10% SDS polyacrylamide gel. Proteins were transferred to PVDF membrane, blocked with 5% milk, probed with primary antibodies and reacted with corresponding secondary antibodies, then detected with the enhanced chemiluminescence system (Millipore, Billerica, MA). Membranes were exposed to an X-ray film to visualize the bands (Amersham Pharmacia Biotech, Piscataway, NJ). Primary antibodies contained Snail (#3879), E-cadherin (#4065), N-cadherin (#4061), Src (#2108), pSrc (Y527, #2105) pAkt (T308, #9275), pAkt (S473, #9271), FAK (#3285), pFAK (Y925, #3284), STAT3 (#9132), pSTAT3 (Y705, #9131), ERK (#9102) and pERK (T202/T204, #9101) which was purchased from Cell Signaling Technology (Beverly, MA), and vimentin (MAB3400), β-tubulin (#05-661) were purchased from Millipore (Billerica, MA), and Fibronectin (sc-8422), pPP2A (sc-12615), were purchased from Santa Cruz Biotechnology Inc. (Santa Cruz, CA), and

cleaved-caspase 3 (1476-1) was purchased from Epitomics (Burlingame, CA).

In vitro migration and invasion assay

Cells were labeled with a vital dye, either CMFDA (green, 492 ex, 516 em, Molecular Probes) or CMTMR (red, 540 ex, 566 em, Molecular Probes; Eugene, OR; http://www.probes.com) at a final concentration of 1-10 mM in pre-warmed Hank's Balanced Salt Solution (HBSS) for 10 min at 37°C. The medium was replaced with pre-warmed medium and incubated for 30 min at 37°C. Cells were then washed three times with PBS, dislodged with 0.5 mM EDTA and dispersed into homogeneous single-cell suspensions in serum-free and phenol red-free DMEM to a concentration of 10^5 cells/300 ml. To assess migration or invasion, a modification of the Boyden chamber method was used. CMFDA-labeled cells (10^5) were added to each insert of 24-Multiwell plate (BD Falcon™ HTS FluroBlock™ Insert System, 8-μm pore size) with or without 100 μl Matrigel (2 mg/ml) (Becton, Dickinson and Company, Billerica, Massachusetts), and 1 ml of phenol red-free DMEM with increasing concentrations of FBS was added to the lower compartments. Migration was allowed to proceed for 14 to 20 h and invasion was allowed to proceed for 24 to 48 h at 37°C. Cells that had migrated to the lower surface of the filter were counted under a fluorescence-equipped microscope at 100× magnifications. The average number of migrating cells per field was assessed by counting at least four random fields per filter. Data points indicate the mean obtained from three separate chambers within one representative experiment.

Spheroid culture assay

For spheroid suspension culture, cancer cells were suspended in a tumorsphere medium consisting of DMEM/F12 (Corning, Manassas, VA), N2 supplement (Gibco Life Technologies, Paisley, UK), human recombinant epidermal growth factor (EGF) (20 ng/mL, PeproTech, Rocky Hill, NJ), and basic fibroblastic growth factor (bFGF) (10 ng/mL, PeproTech) in the ultra-low dish (Corning, Manassas, VA). Formation of spheres, defined as cell colonies >50 μm in diameter and >50% in an area showing a 3-dimensional structure and blurred cell margins [18], was assessed at indicated time periods.

TUNEL assay for suspension apoptosis

Detection of apoptosis in spheroid suspension culture was performed at 48 h according to the manufacturer's instructions (Roche Molecular Biochemicals, Indianapolis, IN). Cells were first fixed with 4% paraformaldehyde, rinsed with PBS, incubated with blocking solution (3% H_2O_2 in methanol) for 10 min, rinsed with PBS, permeabilized by 0.1% Triton X-100 in 0.1% sodium citrate for 2 min at 4°C, and incubated with reaction mixture for 60 min at 37°C in the dark. Then the cells were rinsed with PBS and counterstained with 4,6-diamidino-2-phenylindole (DAPI). Immunofluorescence was observed with fluorescence microscope.

Transfection of gene overexpression constructs

The pCMV-Tag 2B-Snail WT or 6SA plasmids were provided by Dr. Mien-Chieh Hung [19]. For transfection of cells with control pmaxGFP or experimental gene silencing or overexpression constructs, Nucleofector technology (AMAXA Biosystems, Cologne, Germany) was used with each nucleofection sample containing 4 μg of DNA, 5×10^5 cells, and 100 μl of Human Cancer Cell Nucleofector Solution. The transfection was carried out under the program C-17 of the Nucleofector device, as described previously [20]. The transfected cells were then suspended in an appropriate volume of 20% FBS supplemented medium and seeded for further culture. After 48 h of incubation, protein was extracted by M-PER Mammalian Protein Extraction Reagent with Halt™ Protease Inhibitor Cocktail Kit for western blot.

Lentiviral production and cell infection

The lentiviral-based expression plasmids, pLOVE-c-Src WT or Y527F plasmids, were obtained by Dr. Dihua Yu from Departments of Molecular and Cellular Oncology, University of Texas M. D. Anderson Cancer Center [21]. Lentiviral production for Src WT or Y527F overexpression were performed by transfection of 293T cells using Lipofectamine 2000 (LF2000; Invitrogen) [22]. Cells were infected in the presence of 8 μg/mL polybrene (Sigma-Aldrich) and selected with puromycin (1 μg/mL).

Transcriptome analysis

Total RNA was isolated using the RNeasy kit (Qiagen, Hilden, Germany). The generation of labelled cRNA and its hybridization to Human U133 Plus 2 GeneChip arrays (Affymetrix, Santa Clara, CA) were carried out at the genomic core facilities in the National Yang-Ming University (Taipei, Taiwan) according to the standard procedures. Functional annotation and identification of over-represented functional themes were performed using Reactome database of GSEA [23]. Data were submitted and approved by Gene Expression Omnibus (GEO; accession number GSE206046).

Quantitative real-time PCR

The method of quantitative real-time RT-PCR was performed as described [26]. Total RNA (2 μg) of each sample reversely transcribed in 20 μl using 0.5 μg of oligo (dT) (Invitrogen, Carlsbad, CA) and 200 U Superscript III RT (Invitrogen, Carlsbad, CA). Amplification was carried out in a total volume of 20 μL, with SYBR Green PCR MasterMix (Applied Biosystems, Foster City, CA), the cDNA and 500 nM of each primer. All of Primer sequences are list in Table S1. The reaction conditions were one cycle at 95°C for 10 min followed by 40 cycles of denaturation at 95°C for 15 sec, annealing at 56°C for 15 sec, and extension at 72°C for 40 sec. Standard curves (cycle threshold values versus template concentration) were prepared for each target gene and for the endogenous reference (GAPDH) in each sample. The quantification of the unknown samples was performed by the ABI Applied Biosystems (Foster City, CA) with StepOne software v2.0.

ChIP-PCR

Expression of 3rd E-box was confirmed by PCR using forward Src primer and as internal control (Table S1). The amplification was carried out in a total volume of 25 μL containing 500 ng genomic DNA, 0.4 μM of each primer, 200 μM dNTP (Takara Biochemicals, Otsu, Japan), 1.5 mM $MgCl_2$ (Roche), 1 U FastStart Taq polymerase (Roche) and 1× PCR reaction buffer (Roche). The entire mixture of 25 μL was subjected to 35 cycles of 1 min denaturation at 95°C, 1 min to allow annealing at 63°C, and 2 min of extension at 72°C. During the last cycle, the extension time was increased by 7 min. Amplified products were analyzed by 1.5% agarose gel electrophoresis

Luciferase activity assay

A 610-bp fragment containing the functional promoter region of the human c-Src gene [24] was cloned into pGL3 Luciferase reporter plasmid (Promega, Madison, Wisconsin). For generation of Src promoters containing mutation sites, site-directed mutagenesis method using PCR was applied. Luciferase assay was performed using the Dual Luciferase Reporter Assay kit, according to the manufacturer's protocol (Promega, Madison, WI, USA). Briefly, MCF7-CV and MCF-6SA cells were cultured in serum-free medium in 96-well assay plates and transfected with 200 ng/well reporter plasmid, plus 20 ng/well control plasmid, Renilla luciferase plasmid (pRL-TK). After 24 hours of incubation, cells were replenished with fresh medium. After 48 hours of treatment luciferase assays were performed. All transient transfections were performed using Lipofectamine 2000 (Invitrogen).

Immunohistochemical staining

Paraffin-embedded tumor blocks including $ER^{+/-}$, $PR^{+/-}$ and $HER2^{+/-}$ samples were provided by Tissue Bank in Taipei VGH after IRB approval (No. 2020-07-025CC). Paraffin-embedded tumor sections were deparaffinized in xylene, dehydrated through graded alcohols, and pretreated with 0.4 mg/ml proteinase K (DAKO, Carpinteria, Calif., USA) in TRIS-HCl for 15 min at room temperature for optimal antigen retrieval. Residual enzymatic activity was removed by washing in phosphate-buffered saline (PBS), and non-specific staining was blocked with PBS containing 10% normal horse serum for 20 min at room temperature. The sections were then reacted with mouse monoclonal antibodies against Src (#2110, Cell Signaling) and vimentin (MAB3400, Millipore) for 1 h at room temperature. After extensive washes with PBS, a secondary antibody of biotinylated horse anti-mouse (1:200; Vector Laboratories, Mass., USA) was placed on the sections for 30 min at room temperature. Immunostaining was detected by Vectastain ABC reagent (Vector Laboratories, Burlingame, Calif., USA), followed by diaminobenzidine staining. Counterstaining was performed with Mayer's hematoxylin.

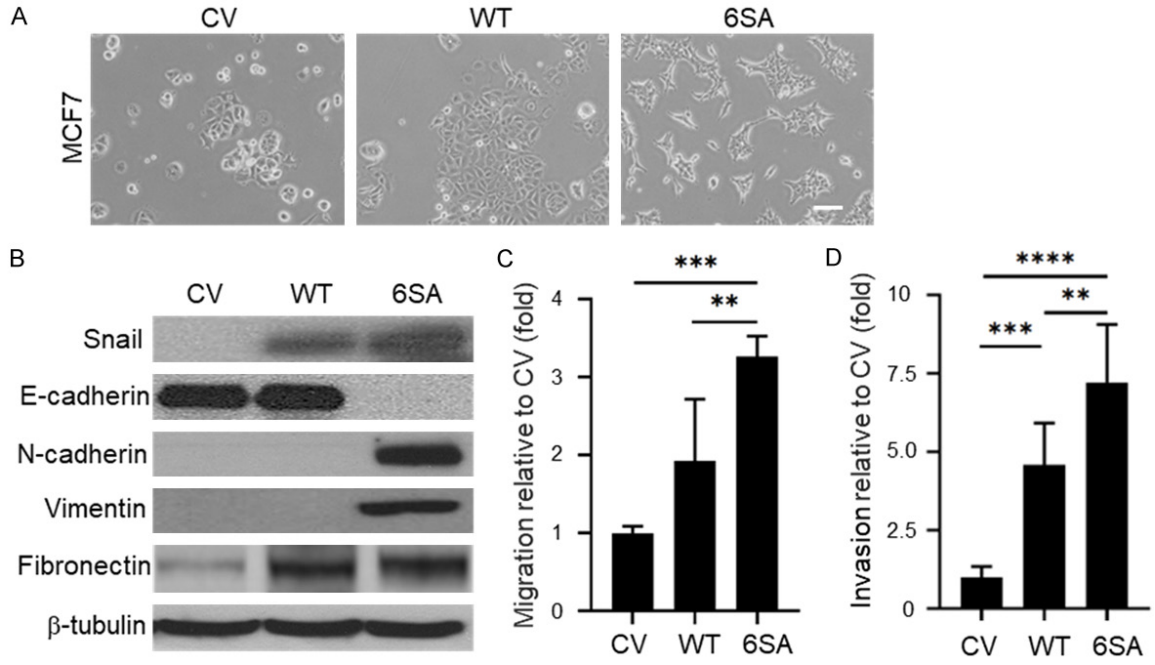

Figure 1. Overexpression of 6SA-Snail in MCF7 increases EMT phenotype. MCF7 cells were transfected with control vector (CV) or vector carrying wildtype (WT) Snail or 6SA-Snail mutant (6SA), followed by (A) morphological observation, (B) analysis of protein expression by western blotting, (C) migration, and (D) invasion assay. The quantification results are shown as mean ± SD. Asterisks indicate significant differences as determined by the One Way ANOVA (**P<0.01, ***P<0.001, ****P<0.0001 versus CV). Scale bar, 100 μm.

Statistical analysis

All values are expressed as mean ± SD. Analysis of variance (ANOVA) and the unpaired student's t-test were used for statistical comparisons in groups greater than and equal to two, respectively (GraphPad Prism 8.0; GraphPad Software, CA). A value of $P<0.05$ is considered to be statistically significant.

Results

EMT-induced by Snail increases migration and invasion of luminal type A breast cancer cells

To investigate the role of EMT in promoting migration, invasion and metastasis of luminal type A breast cancer cells, we overexpressed an active mutant of Snail, 6SA-Snail, which has been demonstrated to be resistant to proteasome-dependent degradation [19]. Luminal type A tumor cell line, MCF7, when overexpressed with 6SA-Snail gene (referred to as MCF7-6SA) adopted the fibroblastic-like morphology (**Figure 1A**), and increased in the expression of EMT markers, such as Vimentin, N-cadherin and Fibronectin, but decreased in the expression of E-cadherin compared to cells overexpressed with control vectors (referred to as MCF7-CV) (**Figure 1B**). Moreover, these cells increased in the capacity of migration (**Figure 1C**) and invasion (**Figure 1D**). As expected, MCF7 cells overexpressed with wild type (WT) Snail gene (referred to as MCF7-WT), which contains the phosphorylation site for ubiquitination [19], did not obviously increase the protein level of Snail and the EMT phenotypes (**Figure 1B-D**). Similar findings were also observed in another luminal type A breast cancer cell line, T47D (Figure S1A-D). These data suggest that Snail-induced EMT increases migration and invasion in luminal type A breast cancer cells.

Snail-induced EMT reduces breast cancer cell colonization and spheroid formation

Because the next step of metastasis following extravasation is colonization [25], we next examined the effect of Snail-induced EMT on colonization ability by using a suspension spheroid culture assay [26, 27]. We observed

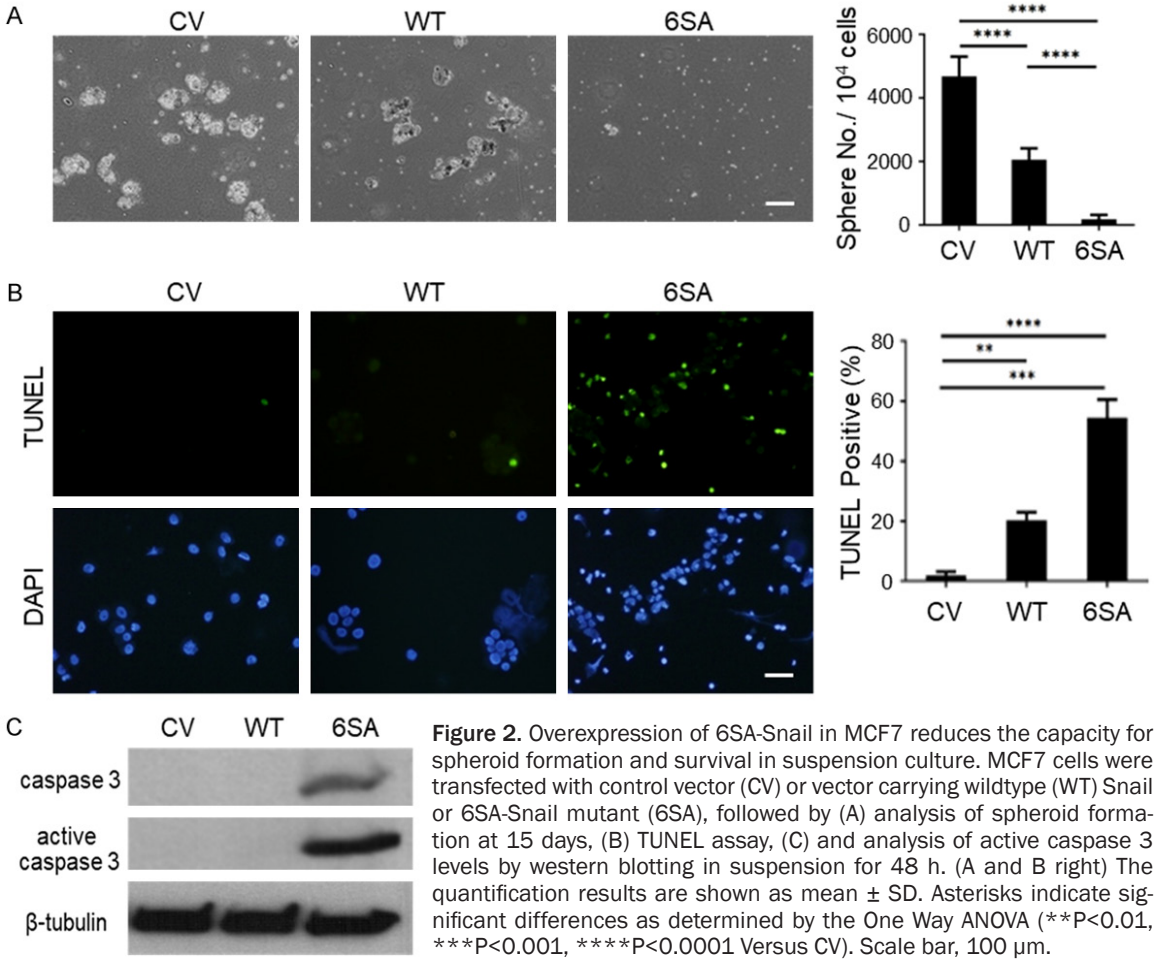

Figure 2. Overexpression of 6SA-Snail in MCF7 reduces the capacity for spheroid formation and survival in suspension culture. MCF7 cells were transfected with control vector (CV) or vector carrying wildtype (WT) Snail or 6SA-Snail mutant (6SA), followed by (A) analysis of spheroid formation at 15 days, (B) TUNEL assay, (C) and analysis of active caspase 3 levels by western blotting in suspension for 48 h. (A and B right) The quantification results are shown as mean ± SD. Asterisks indicate significant differences as determined by the One Way ANOVA (**P<0.01, ***P<0.001, ****P<0.0001 Versus CV). Scale bar, 100 μm.

that MCF7-CV and MCF7-WT but not MCF7-6SA cells formed spheres in suspension culture (**Figure 2A**), suggesting Snail-induced EMT decreases colonization in luminal type A breast cancer cells. The ability to survive in suspension culture is a key factor in determining colonization of cancer stem cells [26, 27]. We thus examined the suspension survival ability for these cells and found that, MCF7-CV and MCF7-WT but not MCF7-6SA survived in suspension culture (**Figure 2B**). T47D cells overexpressed with 6SA-Snail also decreased in sphere formation and suspension survival, compared to cells overexpressed with control vector (Figure S2A, S2B). Moreover, the decreased suspension survival in MCF7-6SA was associated with an increased level of active caspase 3 (**Figure 2C**). Together these data suggest that Snail-induced EMT reduces the suspension viability of luminal A breast cancer cells, thereby inhibiting their colonization and spheroid formation.

Snail induces apoptosis in suspension conditions via Src downregulation

There are many mechanisms or molecules that drive DCCs to colonize distant tissues, including BMP antagonists [28, 29], MET inducers [30], factors suppressing EMT inducer, such as Prxx1 [6], loss of dependency on anchorage for growth [31], activation of stem cell signaling [32, 33], and metabolic reprogramming [34, 35]. To elucidate the downstream signaling by which 6SA-Snail suppresses colonization, we first compared the expression profiles of MCF7-CV and MCF7-6SA with the use of microarray data. Through gene set enrichment analysis (GSEA), we found that several pathways were upregulated or downregulated in MCF7-6SA, compared to MCF7-CV (Figure S3A). Of these, estrogen-dependent gene expression and estrogen receptor (ESR)-mediated signaling were among the most downregulated pathways in MCF7-6SA (Figure S3B), which may contribute to the previously observed phenotypic changes

in these ER+ cancer cell lines. Interestingly, Src, an important colonization master gene that plays an important role in distant metastasis of luminal A breast cancer [36], was listed in ESR-mediated signaling and downregulated in MCF7-6SA (Figure S3C). We further confirmed that 6SA-Snail downregulated Src both as mRNA (**Figure 3A**) and protein levels (**Figure 3B**). However, phosphorylation levels of Akt at serine 308 and threonine 473 were increased in MCF7-6SA compared to MCF7-CV, suggesting that Akt, an important factor for supporting cancer stemness and sphere formation in other cancer types [37, 38], did not play a role in suspension survival and sphere formation of MCF7. We then examined whether overexpressing a WT or an active mutant of Src, Y527F (**Figure 5A**), could overcome 6SA-Snail-induced apoptosis and reduction in sphere formation in suspension condition. Overexpression of either WT or Y527F mutated Src in MCF7-6SA decreased apoptosis in suspension condition, while the degree of reduction in apoptosis was greater with Y527F mutated Src than WT Src (**Figure 3C**). However, there was no effect of overexpression of both constructs on the inhibition of apoptosis in MCF7-CV. Furthermore, both of overexpression with WT or Y527F mutated Src induced an increase in sphere formation (**Figure 3D**). Moreover, we observed a more pronounced degree of colonization capacity and increased suspension sphere formation *in vitro* with Y527F Src compared to WT Src (**Figure 3D**). Notably, both of WT or Y527F mutated Src did not induce changes in the protein levels of EMT markers in MCF7-6SA (Figure S4). These data suggest that Src behaves as a downstream signaling of Snail and is important for the suspension survival, sphere formation and *in vitro* colonization ability.

Snail inhibits Src promoter activity

We then examined whether Snail downregulates Src through direct binding to the promoter of Src. We found that the four putative E-box binding DNA motifs (CANNTC) that Snail may bind in the promoter of Src (**Figure 4A**). Using chromatin immunoprecipitation (ChIP)-PCR (**Figure 4B**) or quantitative PCR (qPCR) assay, we demonstrated that 6SA-Snail bound to the 3rd E-box (**Figure 4C**). Overexpression of 6SA-Snail greatly inhibited the luciferase activity of the Src promoter construct (**Figure 4D**). Moreover, overexpression of two constructs that contained mutated 3rd Src E-box reduced 6SA-Snail-mediated suppression of luciferase activity (**Figure 4E**). These data suggest that Snail downregulates Src through direct binding to its promoter.

Src regulates the phosphorylation of FAK, ERK and STAT3

To understand the mechanism by which Src, a tyrosine kinase, mediates the increase of suspension survival and colonization, we further screened the phosphorylation levels of several important signaling molecules. As mentioned previously, we found that 6SA-Snail induced the downregulation of Src, but more interestingly, we found that Snail suppressed the phosphorylation levels of FAK (Y925), ERK (T202/Y204) and STAT3 (Y705). Furthermore, simultaneous overexpression of WT or Y527F Src mutant overcame 6SA-Snail-mediated dephosphorylation of FAK, ERK and STAT3 (**Figure 5A**). Similar data were obtained for T47D luminal type A cancer cell line (Figure S5A). As expected, inhibition of Src activity by Src family kinase inhibitor PP2 [39] also dephosphorylated FAK, ERK and STAT3 (**Figure 5B**). In addition, inhibition of Src, ERK and STAT3 with PP2, U0126 [40] and S31-201 [41], respectively, also suppressed suspension survival and sphere formation of MCF7-CV (**Figure 5C**, **5D**) and T47D-CV (Figure S5B, S5C). Together, these data suggest that Src plays an important role in suspension survival and sphere formation via phosphorylation of FAK, ERK and STAT3 in luminal type A breast cancer cells.

Downregulation of Src by Snail was not observed in breast cancer cells other than luminal type A

To examine whether downregulation of Src by Snail found in luminal type A breast cancer cells was also observed in other breast cancer cell type, we overexpressed 6SA-Snail in BT474, a luminal type B cell line, AU565, an ERBB2+ cell line, and MDA-MB231, a triple negative cell line. Overexpression of 6SA-Snail caused a slight morphological change (data not shown) and increased sphere formation ability (**Figure 6B**). However, protein (**Figure 6A**) and mRNA (**Figure 6C**) levels, as well as promoter activity of Src (**Figure 6D**), did not change with

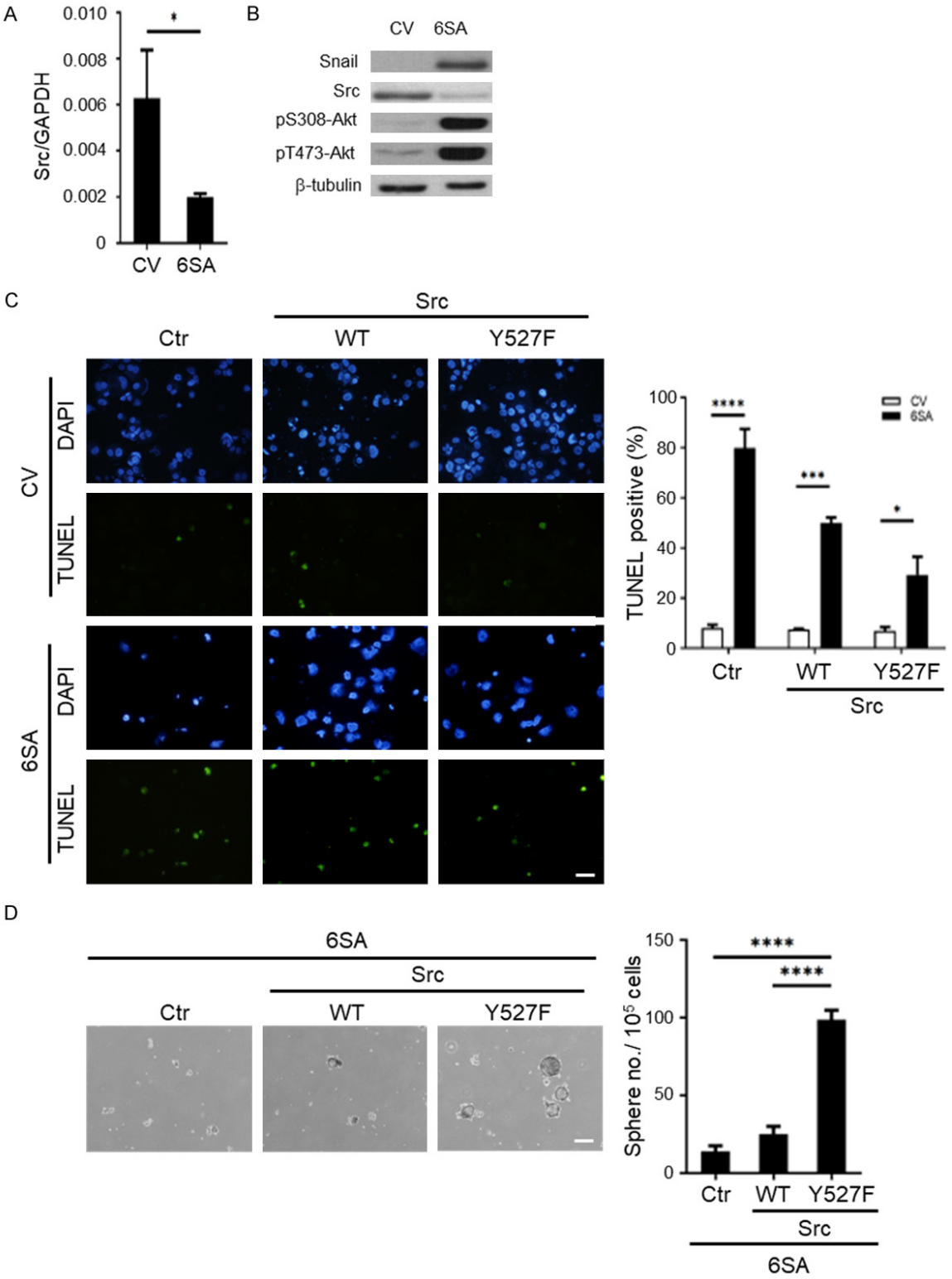

Figure 3. Overexpression of 6SA-Snail in MCF7 induces apoptosis in suspension culture via Src downregulation. MCF7 cells were transfected with control vector (CV) or vector carrying 6SA-Snail mutant (6SA), followed by (A) analysis of mRNA expression by real-time RT-PCR, (B) and analysis of protein levels by western blotting. (C, D) MCF7 cells transfected with control vector (CV) or vector carrying 6SA-Snail mutant, were further transfected with control vector (Ctr), vector carrying wildtype (WT) Src or SrcY527F mutant, and subjected to (C) TUNEL assay in suspension culture for 48 h, and (D) spheroid formation at 15 days. (C and D right) The quantification results are shown as mean ± SD. Asterisks indicate significant differences as determined by the One Way ANOVA (*P<0.05, ***P<0.001, ****P<0.0001 versus CV or Ctr). Scale bar, 100 μm.

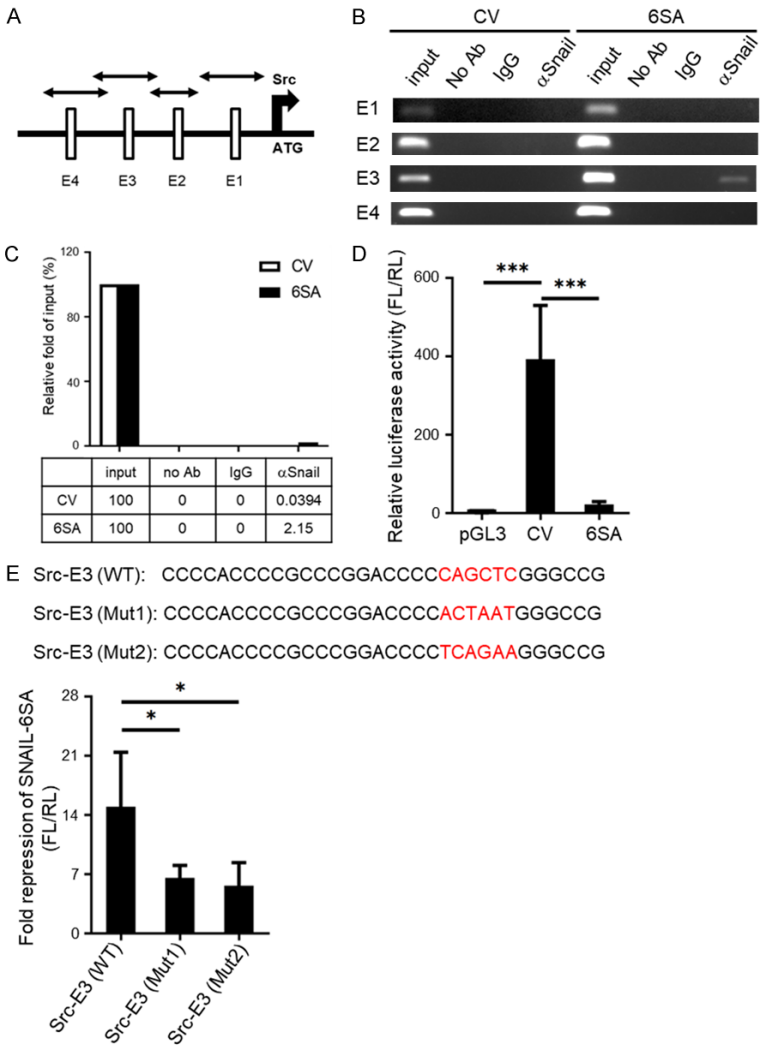

Figure 4. Snail reduces Src expression through direct binding to the 3rd E-box. (A) The illustration for the four proximal E-boxes locating close to the Scr core promoter. Regions flanked by paired primer sets are indicated by double-headed arrows. ATG indicates Transcription start site. (B, C) MCF7 cells were transfected with control vector (CV) or vector carrying 6SA-Snail mutant (6SA), followed by (B) ChIP-PCR or (C) ChIP-qPCR assay. The chromatin was incubated without or with antibodies against Snail, or its isotype IgG antibodies. Fragments of E1, E2, E3, and E4 on the Src promoter were amplified by (B) PCR and (C) qPCR (upper) and its quantification (lower). The results are mean of three independent experiments. (D) Luciferase assay showing that 6SA-Snail decreased the Src promoter activity in MCF7 cell line (n=3). (E) The repressive activity of 6SA-Snail binding 3rd-E box were confirmed with two mutants of 3rd-E box by luciferase assay. The quantification results are shown as mean ± SD. Asterisks indicate significant differences as determined by the One Way ANOVA (*P<0.05, ***P<0.001 versus CV or WT).

overexpression of 6SA-Snail. Similar findings were also observed in another non-luminal type A breast cancer cell line, MDA-MB-231 (Figure S6). These data suggestthat downregulation of Src by Snail was not found in breast cancer cell types other than luminal type A.

Inverse correlation between Src and a mesenchymal marker expression in patient samples of luminal type A breast cancer

To extend the finding that Snail regulates Src expression levels in luminal A breast cancer cell lines, we further analyzed some human luminal A breast cancer samples by immunohistochemical analysis. As known in the literature [19], Snail is unfortunately not suitable for histological evaluation due to its greater instability. Instead, we examined the correlation between Src and the mesenchymal marker Vimentin, one of the downstream targets of Snail-induced EMT [42]. Strikingly, Src and Vimentin were found to be inversely correlated in these set of samples (**Figure 7A**). Interestingly, we also observed a transition of Src^+/$Vimentin^-$ (epithelial status) to Src^-/$Vimentin^+$ (mesenchymal status) or Src^-/$Vimentin^-$ as breast cancer staging progressed from stage I to III (**Figure 7B**). Taken together, these data demonstrate an inverse correlation between the expression of Src and the expression of mesenchymal markers in luminal A breast cancer patient samples.

Discussion

In the current study, we demonstrated that luminal type A tumor such as MCF7 and T47D when overexpressed with active mutant form of Snail gene increased in the expression of EMT markers, such as Vimentin, and N-cadherin but decreased in the expression of E-cadherin compared to cells overexpressed with control vectors or wild type Snail gene. Moreover, these cells increased in the capacity of migration and

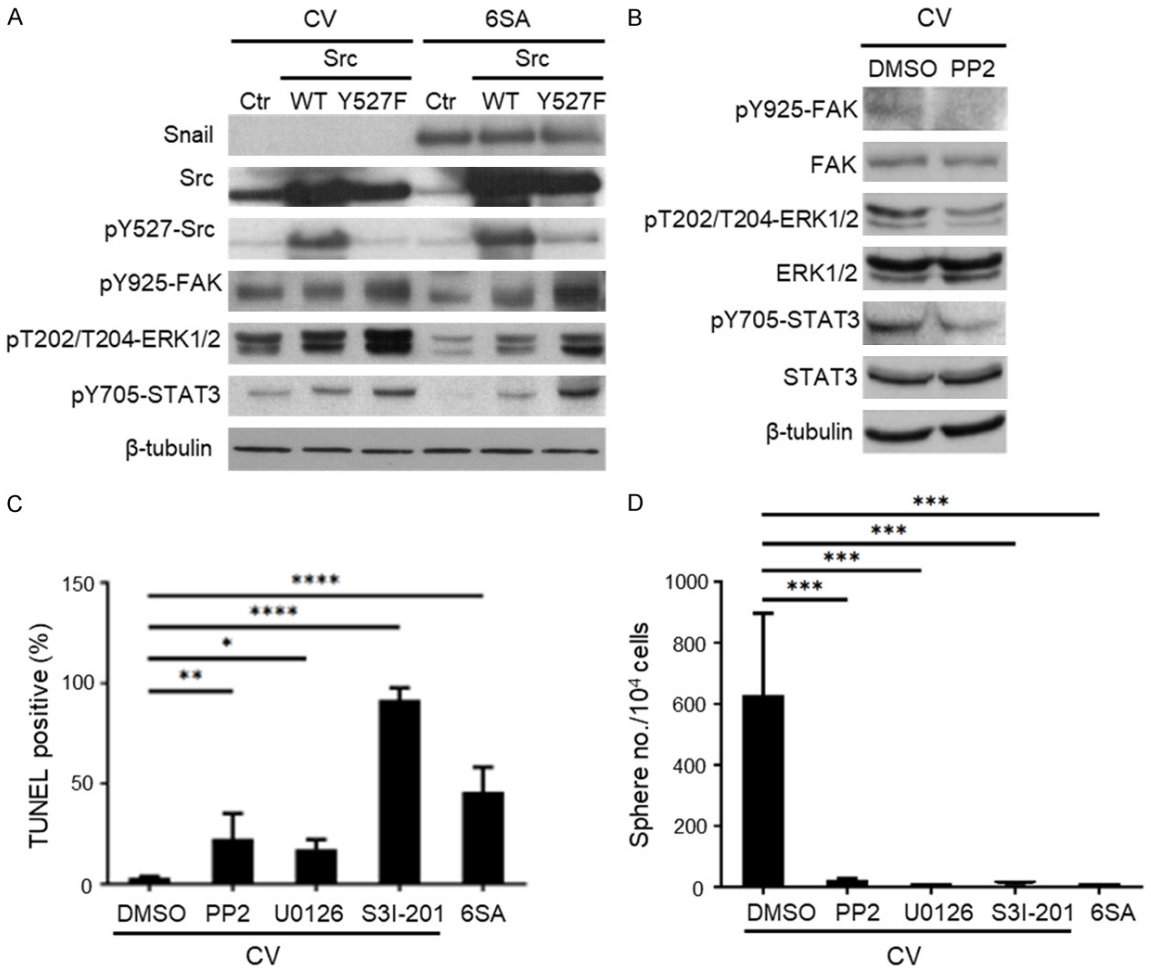

Figure 5. Overexpression of 6SA-Snail in MCF7 induces apoptosis in suspension culture via downregulation of Src downstream pathways. MCF7 cells were transfected with control vector (CV) or vector carrying 6SA-Snail mutant (6SA), further transfected with control vector (Ctr), vector carrying wildtype (WT) Src or SrcY527F mutant, and subjected to (A) western blotting analysis. (B-D) Furthermore, control cells were treated with PP2 (10 μM), U0126 (20 μM) or S3I-201 (100 μM), and subjected to (B) western blotting analysis, (C) TUNEL assay in suspension culture for 48 h, and (D) analysis of spheroid formation at 15 days. The quantification results are shown as mean ± SD. Asterisks indicate significant differences as determined by the One Way ANOVA (*P<0.05, **P<0.01, ***P<0.001, ****P<0.0001 versus CV). Scale bar, 100 μm.

invasion. In contrast, MCF7 or T47D overexpressed with active Snail had reduced ability to survive and form spheroids in serum-free medium.

The mechanism is that down-regulation of Src by Snail affects *in vitro* colonization of Luminal type A breast cancer; however, Snail-mediated down-regulation of Src was not found in other breast cancer cell types, such as BT474 luminal type B, ERBB2^{+} AU565, and triple negative MDA-MB-231 cells. The current study successfully identified the molecular mechanism or signaling pathways involved in controlling dormancy in luminal type A breast cancer, and help explaining the differences of latency period in different subtypes of breast cancer.

Here, we found that luminal type A breast cancer cells when overexpressed with active mutant Snail but not wild type Snail, acquired EMT phenotypes, including the expression of EMT markers, increased migration and invasion. Our data reproduce previous findings that wild type Snail is sensitive to protease-dependent degradation [19] and also reinforce the concept that EMT is responsible for invasion and early dissemination of primary tumor, generating DCCs in distant organs. Our data are the first to demonstrate that a master regulator

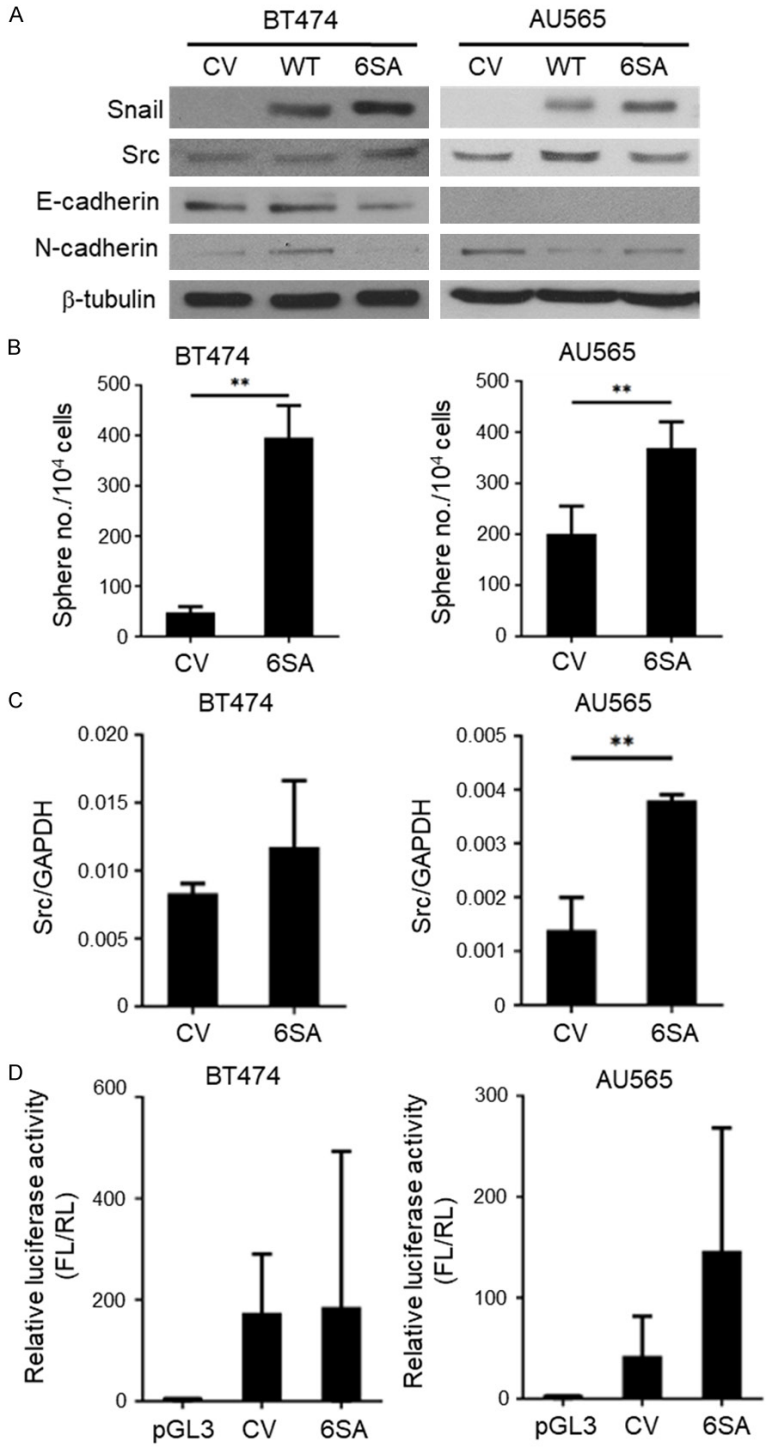

Figure 6. Overexpression of 6SA-Snail in BT474 and Au565 does not reduce spheroid formation in suspension culture, or induce Src downregulation. BT474 and Au565 cells transfected with control vector (CV) or vector carrying wildtype (WT) Snail or 6SA-Snail mutant (6SA), followed by (A) protein expression by western blotting, (B) spheroid formation in suspension culture at 15 days, (C) analysis of Src mRNA expression by real-time RT-PCR, and (D) Luciferase assay for the repressive activity of 6SA-Snail on Src promoter. The quantification results are shown as mean ± SD. Asterisks indicate significant differences as determined by the unpaired Student's t-test (**P<0.01 versus CV).

of MET, Src [36], is directly inhibited by EMT inducer, Snail. Compared to other EMT transcription factors (TFs), Snail is the EMT trigger, while other EMT-TFs, such as Twist1, reinforce and maintain the mesenchymal state [43-45]. Interestingly, downregulation of Src by EMT inducer was only observed in Snail but not in Twist1, further suggesting that Snail is a major regulator between EMT and MET.

The involvement of EMT in metastasis is still controversial, due to the invariable display of epithelial features, such as well-organized adhesion junctions, and the lack of a mesenchymal phenotype in human carcinoma metastases [17]. These data suggest tumor cells that have disseminated via acquiring EMT need to revert to an epithelial phenotype to form macrometastases. In a spontaneous squamous cell carcinoma mouse model, expression of Twist promotes tumor cell invasion and dissemination, however, spatiotemporal inactivation of this factor is essential for inducing metastasis [46]. BT-549 human breast cancer cells express Prrx1 and Twist1 but not Snail to induce EMT. However, when BT-549 cells were injected into the tail vein of immunocompromised mice, they colonized the lungs and induced metastasis, which required Prrx1 silencing to revert EMT to MET [6]. However, the downstream pathway of Prxx1 responsible for EMT-MET reversal has not been well explored. In contrast, we found that when Snail was expressed, MCF7 lost its ability to colonize distant tissues

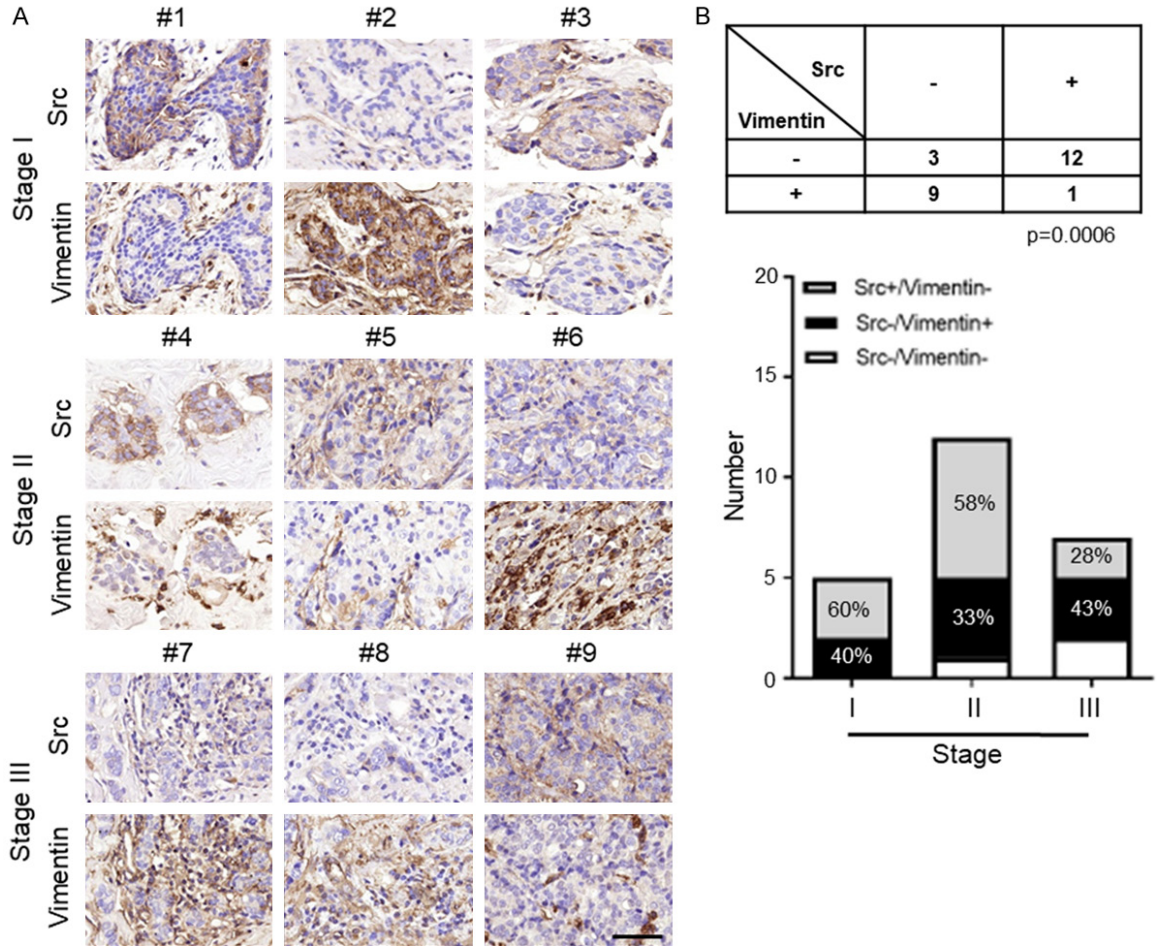

Figure 7. Expression of Src and Vimentin are inversely correlated in clinical samples of luminal type A breast cancer. Luminal A breast cancer patient samples were assayed for Src and Vimentin expression by immunohistochemistry (n=25). A. Representative pictures showing (Upper) Src and (Lower) Vimentin expression in stage I, II and III patient samples. B. Quantitative data are shown. Significant difference (P=0.0006) as determined by the two-sided Mann-Whitney U-test. Scale bar, 50 μm.

by suppressing the expression of Src, the master gene of MET [36].

Similarly, the mechanism of early dissemination and metastasis in $Her2^{+}$ mammary cancer has been identified [47]. In MMTV-Her2 mice, a sub-population of invasive $Her2^{+}$ p-$p38^{lo}$ p-$Atf2^{lo}$ $Twist1^{hi}$ E-cad^{lo} early disseminated cancer cells (eDCCs) are non-replicative and quiescent, whereas DCCs found in animals with overt tumors are replicative, suggesting that eDCCs remain dormant and require downregulation of Twist for release from dormancy. In BALB-NeuT mice, a large proportion of metastases are derived from eDCC ancestors, whose migration was triggered by progesterone-induced signaling shortly after HER2 activation [48]. Interestingly, cells from early-stage, low-density lesions exhibited more stemness features, more migration, and more metastasis than cells from dense, advanced tumors with increased proliferation.

In conclusion, we showed in luminal type A breast cancer that when cells acquired an EMT phenotype, especially caused by Snail, they decreased the expression of the MET master gene Src, lost the ability to colonize, and became long-term dormant cells. These data may help to explain the long latency of luminal breast cancer in cancer progression [1], and to develop new strategies to prevent recurrence and metastasis.

Acknowledgements

This work was supported by the “Drug Development Center, China Medical University”

from The Featured Areas Research Center Program within the framework of the Higher Education Sprout Project by the Ministry of Education (MOE) in Taiwan. This work was financially supported by Minister of Science and Technology (MOST 109-2314-B-039-009-MY3). China Medical University (CMU110-Z-05), and China Medical University Hospital (DMR-108-BC-5). The funding sources had no involvement in study design, in the collection, analysis and interpretation of data, in the writing of the report, and in the decision to submit the article for publication.

Disclosure of conflict of interest

None.

Address correspondence to: Dr. Mien-Chie Hung, Office of The President, China Medical University, 100, Sec. 1, Jingmao Rd., Beitun Dist., Taichung 406, Taiwan. Tel: +886-4-22057153; Fax: +886-4-22952121; E-mail: mhung@cmu.edu.tw; Dr. Shih-Chieh Hung, Distinguished Professor, Institute of New Drug Development, Taichung, Taiwan; Director, Drug Development Center, China Medical University, No.91 Hsueh-Shih Road, North District, Taichung 40402, Taiwan. Tel: +886-4-2205-2121#7728; Fax: +886-4-2233-3922; E-mail: hung3340@gmail.com; hungsc@cmu.edu.tw

References

[1] Kennecke H, Yerushalmi R, Woods R, Cheang MC, Voduc D, Speers CH, Nielsen TO and Gelmon K. Metastatic behavior of breast cancer subtypes. J Clin Oncol 2010; 28: 3271-3277.

[2] Rajan A, Varghese GR, Yadev I, Anandan J, Latha NR, Patra D, Krishnan N, Kuppusamy K, Warrier AV, Bhushan S, Nadhan R, Ram Kumar RM and Srinivas P. Modulation of BRCA1 mediated DNA damage repair by deregulated ER-alpha signaling in breast cancers. Am J Cancer Res 2022; 12: 17-47.

[3] Zhuang Y, Yang G, Wu S, Chen J, Guo J, Quan D, Zhang T, Yang Z, Tan S, Ji Y, Chen Z and Lv L. 5-arylalkynyl-2-benzoyl thiophene: a novel microtubule inhibitor exhibits antitumor activity without neurological toxicity. Am J Cancer Res 2022; 12: 229-246.

[4] Fidler IJ and Kripke ML. Metastasis results from preexisting variant cells within a malignant tumor. Science 1977; 197: 893-895.

[5] Kalluri R and Weinberg RA. The basics of epithelial-mesenchymal transition. J Clin Invest 2009; 119: 1420-1428.

[6] Ocana OH, Corcoles R, Fabra A, Moreno-Bueno G, Acloque H, Vega S, Barrallo-Gimeno A, Cano A and Nieto MA. Metastatic colonization requires the repression of the epithelial-mesenchymal transition inducer Prrx1. Cancer Cell 2012; 22: 709-724.

[7] Karrison TG, Ferguson DJ and Meier P. Dormancy of mammary carcinoma after mastectomy. J Natl Cancer Inst 1999; 91: 80-85.

[8] Manjili MH. Tumor dormancy and relapse: from a natural byproduct of evolution to a disease state. Cancer Res 2017; 77: 2564-2569.

[9] Aguirre-Ghiso JA. Models, mechanisms and clinical evidence for cancer dormancy. Nat Rev Cancer 2007; 7: 834-846.

[10] Sosa MS, Bragado P and Aguirre-Ghiso JA. Mechanisms of disseminated cancer cell dormancy: an awakening field. Nat Rev Cancer 2014; 14: 611-622.

[11] Giancotti FG. Mechanisms governing metastatic dormancy and reactivation. Cell 2013; 155: 750-764.

[12] Rhim AD, Mirek ET, Aiello NM, Maitra A, Bailey JM, McAllister F, Reichert M, Beatty GL, Rustgi AK, Vonderheide RH, Leach SD and Stanger BZ. EMT and dissemination precede pancreatic tumor formation. Cell 2012; 148: 349-361.

[13] Moody SE, Perez D, Pan TC, Sarkisian CJ, Portocarrero CP, Sterner CJ, Notorfrancesco KL, Cardiff RD and Chodosh LA. The transcriptional repressor Snail promotes mammary tumor recurrence. Cancer Cell 2005; 8: 197-209.

[14] Yang J, Mani SA, Donaher JL, Ramaswamy S, Itzykson RA, Come C, Savagner P, Gitelman I, Richardson A and Weinberg RA. Twist, a master regulator of morphogenesis, plays an essential role in tumor metastasis. Cell 2004; 117: 927-939.

[15] Scheel C, Eaton EN, Li SH, Chaffer CL, Reinhardt F, Kah KJ, Bell G, Guo W, Rubin J, Richardson AL and Weinberg RA. Paracrine and autocrine signals induce and maintain mesenchymal and stem cell states in the breast. Cell 2011; 145: 926-940.

[16] Jayathirtha M, Neagu AN, Whitham D, Alwine S and Darie CC. Investigation of the effects of overexpression of jumping translocation breakpoint (JTB) protein in MCF7 cells for potential use as a biomarker in breast cancer. Am J Cancer Res 2022; 12: 1784-1823.

[17] Chaffer CL and Weinberg RA. A perspective on cancer cell metastasis. Science 2011; 331: 1559-1564.

[18] Liu CC, Li HH, Lin JH, Chiang MC, Hsu TW, Li AF, Yen DH, Hsu HS and Hung SC. Esophageal cancer stem-like cells resist ferroptosis-induced cell death by active Hsp27-GPX4 pathway. Biomolecules 2021; 12: 48.

[19] Zhou BP, Deng J, Xia W, Xu J, Li YM, Gunduz M and Hung MC. Dual regulation of Snail by GSK-3beta-mediated phosphorylation in control of epithelial-mesenchymal transition. Nat Cell Biol 2004; 6: 931-940.
[20] Lin SP, Chiu FY, Wang Y, Yen ML, Kao SY and Hung SC. RB maintains quiescence and prevents premature senescence through upregulation of DNMT1 in mesenchymal stromal cells. Stem Cell Reports 2014; 3: 975-986.
[21] Zhang S, Huang WC, Zhang L, Zhang C, Lowery FJ, Ding Z, Guo H, Wang H, Huang S, Sahin AA, Aldape KD, Steeg PS and Yu D. SRC family kinases as novel therapeutic targets to treat breast cancer brain metastases. Cancer Res 2013; 73: 5764-5774.
[22] Lin SP, Lee YT, Yang SH, Miller SA, Chiou SH, Hung MC and Hung SC. Colon cancer stem cells resist antiangiogenesis therapy-induced apoptosis. Cancer Lett 2013; 328: 226-234.
[23] Subramanian A, Tamayo P, Mootha VK, Mukherjee S, Ebert BL, Gillette MA, Paulovich A, Pomeroy SL, Golub TR, Lander ES and Mesirov JP. Gene set enrichment analysis: a knowledge-based approach for interpreting genome-wide expression profiles. Proc Natl Acad Sci U S A 2005; 102: 15545-15550.
[24] Bonham K and Fujita DJ. Organization and analysis of the promoter region and 5' noncoding exons of the human c-src proto-oncogene. Oncogene 1993; 8: 1973-1981.
[25] Nguyen DX, Bos PD and Massague J. Metastasis: from dissemination to organ-specific colonization. Nat Rev Cancer 2009; 9: 274-284.
[26] Balaji P, Murugadas A, Ramkumar A, Thirumurugan R, Shanmugaapriya S and Akbarsha MA. Characterization of Hen's egg white to use it as a novel platform to culture three-dimensional multicellular tumor spheroids. ACS Omega 2020; 5: 19760-19770.
[27] Liu CC, Lin SP, Hsu HS, Yang SH, Lin CH, Yang MH, Hung MC and Hung SC. Suspension survival mediated by PP2A-STAT3-Col XVII determines tumour initiation and metastasis in cancer stem cells. Nat Commun 2016; 7: 11798.
[28] Song KH, Park MS, Nandu TS, Gadad S, Kim SC and Kim MY. GALNT14 promotes lung-specific breast cancer metastasis by modulating self-renewal and interaction with the lung microenvironment. Nat Commun 2016; 7: 13796.
[29] Gao H, Chakraborty G, Lee-Lim AP, Mo Q, Decker M, Vonica A, Shen R, Brogi E, Brivanlou AH and Giancotti FG. The BMP inhibitor Coco reactivates breast cancer cells at lung metastatic sites. Cell 2012; 150: 764-779.
[30] Stankic M, Pavlovic S, Chin Y, Brogi E, Padua D, Norton L, Massague J and Benezra R. TGF-beta-Id1 signaling opposes Twist1 and promotes metastatic colonization via a mesenchymal-to-epithelial transition. Cell Rep 2013; 5: 1228-1242.
[31] Roe JS, Hwang CI, Somerville TDD, Milazzo JP, Lee EJ, Da Silva B, Maiorino L, Tiriac H, Young CM, Miyabayashi K, Filippini D, Creighton B, Burkhart RA, Buscaglia JM, Kim EJ, Grem JL, Lazenby AJ, Grunkemeyer JA, Hollingsworth MA, Grandgenett PM, Egeblad M, Park Y, Tuveson DA and Vakoc CR. Enhancer reprogramming promotes pancreatic cancer metastasis. Cell 2017; 170: 875-888, e820.
[32] Oskarsson T, Acharyya S, Zhang XH, Vanharanta S, Tavazoie SF, Morris PG, Downey RJ, Manova-Todorova K, Brogi E and Massague J. Breast cancer cells produce tenascin C as a metastatic niche component to colonize the lungs. Nat Med 2011; 17: 867-874.
[33] Gao H, Chakraborty G, Zhang Z, Akalay I, Gadiya M, Gao Y, Sinha S, Hu J, Jiang C, Akram M, Brogi E, Leitinger B and Giancotti FG. Multi-organ site metastatic reactivation mediated by non-canonical discoidin domain receptor 1 signaling. Cell 2016; 166: 47-62.
[34] Loo JM, Scherl A, Nguyen A, Man FY, Weinberg E, Zeng Z, Saltz L, Paty PB and Tavazoie SF. Extracellular metabolic energetics can promote cancer progression. Cell 2015; 160: 393-406.
[35] Dong C, Yuan T, Wu Y, Wang Y, Fan TW, Miriyala S, Lin Y, Yao J, Shi J, Kang T, Lorkiewicz P, St Clair D, Hung MC, Evers BM and Zhou BP. Loss of FBP1 by Snail-mediated repression provides metabolic advantages in basal-like breast cancer. Cancer Cell 2013; 23: 316-331.
[36] Zhang XH, Wang Q, Gerald W, Hudis CA, Norton L, Smid M, Foekens JA and Massague J. Latent bone metastasis in breast cancer tied to Src-dependent survival signals. Cancer Cell 2009; 16: 67-78.
[37] Hsu HS, Liu CC, Lin JH, Hsu TW, Hsu JW, Li AF and Hung SC. Involvement of collagen XVII in pluripotency gene expression and metabolic reprogramming of lung cancer stem cells. J Biomed Sci 2020; 27: 5.
[38] Liu CC, Chou KT, Hsu JW, Lin JH, Hsu TW, Yen DH, Hung SC and Hsu HS. High metabolic rate and stem cell characteristics of esophageal cancer stem-like cells depend on the Hsp27-AKT-HK2 pathway. Int J Cancer 2019; 145: 2144-2156.
[39] Nam JS, Ino Y, Sakamoto M and Hirohashi S. Src family kinase inhibitor PP2 restores the E-cadherin/catenin cell adhesion system in human cancer cells and reduces cancer metastasis. Clin Cancer Res 2002; 8: 2430-2436.
[40] Fukazawa H, Noguchi K, Murakami Y and Uehara Y. Mitogen-activated protein/extracellular signal-regulated kinase kinase (MEK) inhibitors restore anoikis sensitivity in human breast cancer cell lines with a constitutively activated

extracellular-regulated kinase (ERK) pathway. Mol Cancer Ther 2002; 1: 303-309.
[41] Jahangiri A, Dadmanesh M and Ghorban K. Suppression of STAT3 by S31-201 to reduce the production of immunoinhibitory cytokines in a HIF1-alpha-dependent manner: a study on the MCF-7 cell line. In Vitro Cell Dev Biol Anim 2018; 54: 743-748.
[42] Zhang W, Feng M, Zheng G, Chen Y, Wang X, Pen B, Yin J, Yu Y and He Z. Chemoresistance to 5-fluorouracil induces epithelial-mesenchymal transition via up-regulation of Snail in MCF7 human breast cancer cells. Biochem Biophys Res Commun 2012; 417: 679-685.
[43] Tran DD, Corsa CA, Biswas H, Aft RL and Longmore GD. Temporal and spatial cooperation of Snail1 and Twist1 during epithelial-mesenchymal transition predicts for human breast cancer recurrence. Mol Cancer Res 2011; 9: 1644-1657.
[44] Casas E, Kim J, Bendesky A, Ohno-Machado L, Wolfe CJ and Yang J. Snail2 is an essential mediator of Twist1-induced epithelial mesenchymal transition and metastasis. Cancer Res 2011; 71: 245-254.
[45] Peinado H, Olmeda D and Cano A. Snail, Zeb and bHLH factors in tumour progression: an alliance against the epithelial phenotype? Nat Rev Cancer 2007; 7: 415-428.
[46] Tsai JH, Donaher JL, Murphy DA, Chau S and Yang J. Spatiotemporal regulation of epithelial-mesenchymal transition is essential for squamous cell carcinoma metastasis. Cancer Cell 2012; 22: 725-736.
[47] Harper KL, Sosa MS, Entenberg D, Hosseini H, Cheung JF, Nobre R, Avivar-Valderas A, Nagi C, Girnius N, Davis RJ, Farias EF, Condeelis J, Klein CA and Aguirre-Ghiso JA. Mechanism of early dissemination and metastasis in Her2(+) mammary cancer. Nature 2016; 540: 588-592.
[48] Hosseini H, Obradovic MM, Hoffmann M, Harper KL, Sosa MS, Werner-Klein M, Nanduri LK, Werno C, Ehrl C, Maneck M, Patwary N, Haunschild G, Guzvic M, Reimelt C, Grauvogl M, Eichner N, Weber F, Hartkopf AD, Taran FA, Brucker SY, Fehm T, Rack B, Buchholz S, Spang R, Meister G, Aguirre-Ghiso JA and Klein CA. Early dissemination seeds metastasis in breast cancer. Nature 2016; 540: 552-558.

Table S1. Primer sets for real-time PCR and ChIP-PCR

Name	Primer sequence	Size (bp)	NCBI reference sequence
Real-time PCR			
Src	F: CCTCGTGCGAGAAAGTGAG	68	NM_005417
	R: TGGCGTTGTCGAAGTCAG		
GAPDH	F: GAAGGTGAAGGTCGGAGTC	206	NM_002046
	R: GAAGATGGTGATGGGATTTC		
ChIP PCR			
1st E-box	F: CAAAGGGCTCAAACGTTACC	215	NC_000020.11
	R: CCCTTTCTCTCTCGATCTGTC		
2nd E-box	F: CGGGAGAGACAGATCGAGAG	163	NC_000020.11
	R: CGGCGGGGAATCCGTCCCCG		
3rd E-box	F: AGGAGGAGGAAGGAGGAAGC	202	NC_000020.11
	R: TAGAAGGTGGGTGGGTTGG		
4th E-box	F: AACCCACCCACCTTCTACG	149	NC_000020.11
	R: TACCGAGCTCTTACGCGTG		

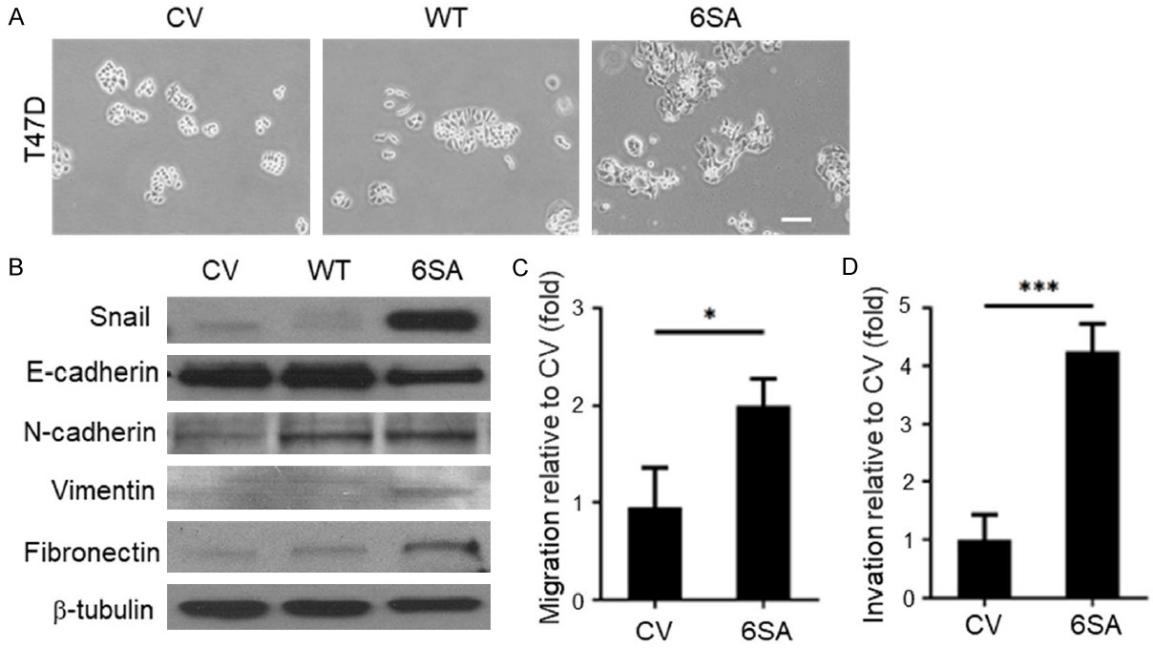

Figure S1. Overexpression of 6SA-Snail in T47D increases EMT phenotype. T47D cells were transfected with control vector (CV) or vector carrying wildtype (WT) Snail or 6SA-Snail mutant (6SA), followed by (A) morphological observation, (B) analysis of protein levels by western blotting, (C) migration, and (D) invasion assay. The quantification results are shown as mean ± SD. Asterisks indicate significant differences as determined by the unpaired Student›s t-test (*p<0.05, ***p<0.001 versus CV). Scale bar, 100 μm.

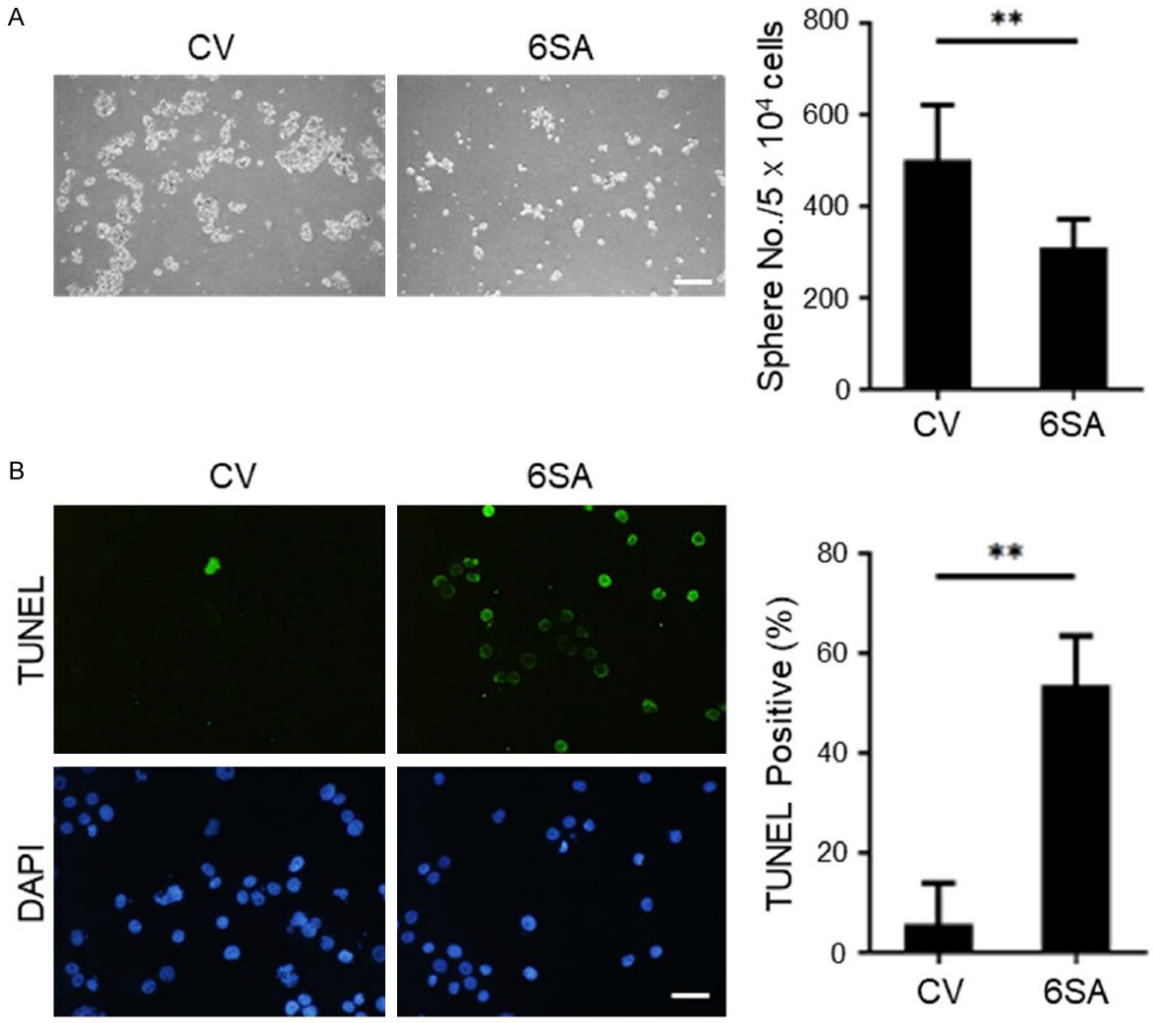

Figure S2. Overexpression of 6SA-Snail in T47D reduces the capacity for spheroid formation, and survival in suspension culture. T47D cells were transfected with control vector (CV) or vector carrying 6SA-Snail mutant (6SA), followed by (A) analysis of spheroid formation at 5 days, (B) TUNEL assay in suspension for 48 h. (A and B Right) The quantification results are shown as mean ± SD. Asterisks indicate significant differences as determined by the unpaired Student›s t-test (**P<0.01 versus CV). Scale bar, 100 μm.

A

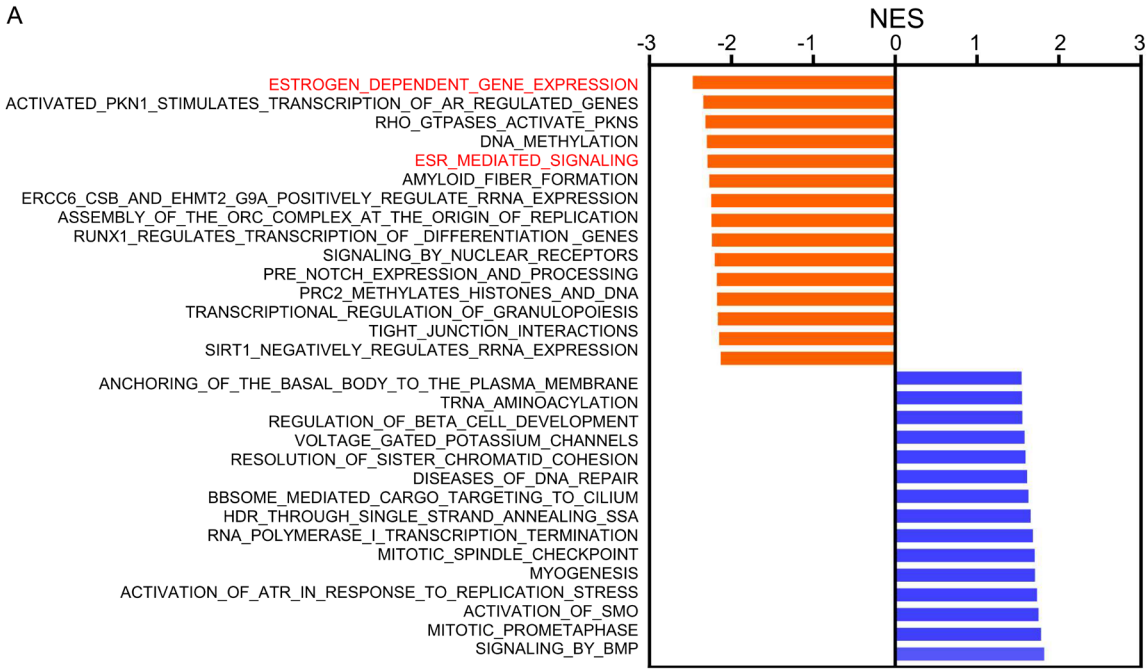

B

C

Down-regulated genes of ESR_MEDIATED_SIGNALING									
NCOA1	DDX5	H4C4	PIK3CA	**SRC**	H3-3B	IGF1R	H2BS1	GNG13	H2AC8
HSP90AA1	EP300	GNG5	PDPK1	PRKCZ	NRAS	AKT1	H2AC7	NCOA3	CXXC5
HDAC1	MOV10	HRAS	BCL2	H2AX	MMP9	H2BC6	BTC	RUNX1	H2AC6
GNB1	ZDHHC21	GNAI3	FKBP4	CALM1	PIK3R2	H2BC4	H3C10	CTSD	
PTK2	UHMK1	KAT5	H4C5	JUND	ZDHHC7	CDK9	CCND1	H2BC5	
HSP90AB1	AGO3	YY1	AKT2	GNAI2	SHC1	GNB5	H3C4	H4C8	
POLR2H	H2AZ1	CARM1	PIK3R3	MAPK3	H4C14	GNB2	H2BC7	ZNF217	
POLR2L	GNGT1	PRMT1	POLR2J	USF2	EREG	NRIP1	MYB	CXCL12	
POLR2I	H3C7	EBAG9	H3C2	H2BC14	H3C6	H2BC10	H2BC9	H2BC8	
CDKN1B	STRN	CREBBP	POLR2G	H4C12	PIK3R1	SPHK1	FOXA1	FOS	
AXIN1	ELK1	KPNA2	H2AZ2	CAV2	TFF1	GATA3	**ESR1**	H2AJ	
CAV1	TGFA	S1PR3	PGR	HSPB1	TFF3	GREB1	H2BC21	AREG	

Figure S3. Gene set enrichment analysis (GSEA) reveals several pathways upregulated or downregulated in MCF7-6SA, compared to MCF7-CV. MCF7 cells were transfected with control vector (CV) or vector carrying 6SA-Snail mutant (6SA), followed by (A) gene expression profile analysis using microarray data and subsequent GSEA pathway analysis to obtain normalized enrichment scores (NES, negative scores indicate downregulated pathways in MCF7-6SA, while positive scores indicate upregulated pathways in MCF7-6SA). (B) Estrogen Dependent Gene Expression and ESR-Mediated Signaling are examples of pathways downregulated in MCF7-6SA compared to MCF7-CV. (C) Downregulated genes of ESR-Mediated Signaling in MCF7-6SA were found through Reactome database analysis.

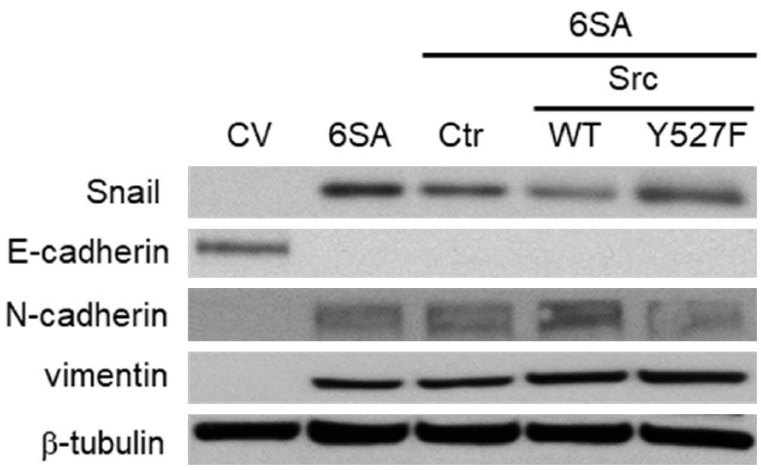

Figure S4. Overexpression of SrcY527F in 6SA-Snail MCF7 does not induce reduction of EMT markers. MCF7 cells transfected with control vector (CV) or vector carrying 6SA-Snail mutant (6SA), were further transfected with control vector (Ctr), vector carrying wildtype (WT) Src or SrcY527F mutant, and followed by analysis of EMT marker expression by western blotting.

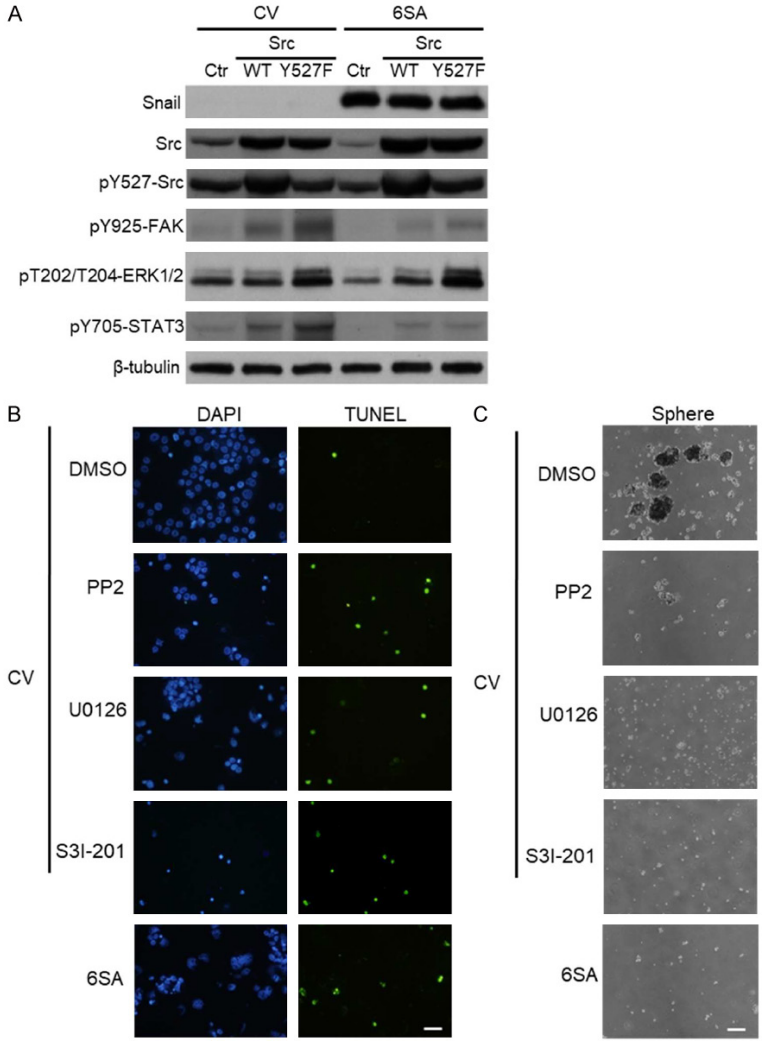

Figure S5. Overexpression of 6SA-Snail in T47D induces apoptosis in suspension culture via Src downregulation. T47D cells transfected with control vector (CV) or vector carrying 6SA-Snail mutant (6SA) were further transfected with control vector (Ctr), vector carrying wildtype (WT) Src or SrcY527F mutant, followed by (A) analysis of protein levels by western blotting. (B, C) Control cells were further treated PP2 (10 μM), U0126 (20 μM) or S3I-201 (100 μM), and subjected to (B) TUNEL assay in suspension culture for 48 h, and (C) spheroid formation at 5 days.

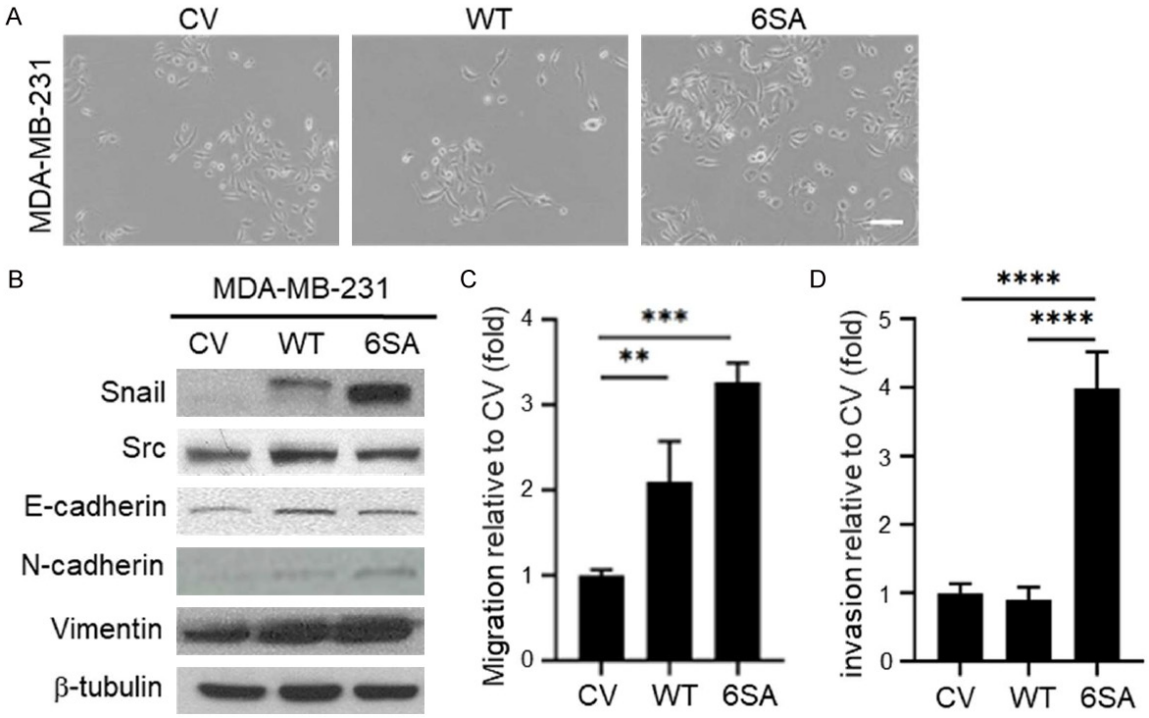

Figure S6. Overexpression of 6SA-Snail in MDA-MB231 does not induce Src downregulation. MDA-MB231 cells transfected with control vector (CV) or vector carrying wildtype (WT) Snail or 6SA-Snail mutant (6SA), followed by (A) morphological observation, (B) analysis of protein levels by western blotting, (C) migration, and (D) invasion assay. The quantification results are shown as mean ± SD. Asterisks indicate significant differences as determined by the One Way ANOVA (**P<0.01, ***p<0.001, ****p<0.0001 versus CV). Scale bar, 100 μm.